ISBN: 978-3-95450-233-2 ISSN: 2673-5504 doi:10.18429/JACoW-SRF2021-TUPTEV013

MANAGING SN-SUPPLY TO TUNE SURFACE CHARACTERISTICS OF VAPOR-DIFFUSION COATING OF Nb_3Sn*

U. Pudasaini†[1], J. Tiskumara[2], C. E. Reece[1]
[1]Thomas Jefferson National Accelerator Facility, Newport News, VA, USA
[2]Old Dominion University, Norfolk, VA, USA

Abstract

Nb_3Sn promises better RF performance (Q and E_{acc}) than niobium at any given temperature because of superior superconducting properties. Nb_3Sn-coated SRF cavities are now produced routinely by growing a few microns thick Nb_3Sn films inside Nb cavities via the tin vapor diffusion technique. Sn evaporation and consumption during the growth process notably affect the quality of the coating. Aiming at favorable surface characteristics that could enhance the RF performance, many coatings were produced by varying Sn sources and temperature profiles. Coupon samples were examined using different material characterization techniques, and a selected few sets of coating parameters were used to coat 1.3 GHz single-cell cavities for RF testing. The Sn supply's careful tuning is essential to manage the microstructure, roughness, and overall surface characteristics of the coating. We summarize the material analysis of witness samples and discuss the performance of several Nb_3Sn-coated single-cell cavities linked to Sn-source characteristics and observed Sn consumption during the film growth process.

INTRODUCTION

Because of superior superconducting properties, Nb_3Sn (T_c ~ 18.3 K, H_{sh} ~ 425 mT, and Δ ~3.1 meV) promises better performance and a significant reduction in operational cost of SRF cavities compared to Nb (T_c ~ 9.2 K, H_{sh} ~ 210 mT, and Δ ~1.45 meV) [1]. Presently, it is the front running alternative material to replace niobium in SRF cavities. However, Nb_3Sn has a significantly lower thermal conductivity despite attractive superconducting properties than Nb at low temperatures. Further, it is very brittle and prone to develop cracks under stress, which primarily restricts the application of Nb_3Sn into a thin film form. Nb_3Sn thin films should be deposited or grown inside a built-in metallic (e.g., Nb, Cu) cavity structure. Since SRF cavities typically have complicated geometries and demand flawless uniform coating, suitable thin film deposition techniques are limited. Among several techniques attempted to deposit Nb_3Sn thin films, vapor diffusion coating is the most favorable and successful technique so far.

Vapor diffusion coating of Nb_3Sn on niobium cavities dates back to the 1970s [2-4]. This technique is adopted by most research institutions currently working to develop Nb_3Sn coated cavities around the world [5-8]. Recent performance results of such cavities are very promising, attaining high quality factors, > 10^{10} operating at 4.2 K at medium fields at ≥ 15 MV/m in several labs [5, 9-10]. A typical cavity coating process consists of two steps: nucleation and growth. First, tin chloride evaporates at about 500 ºC, depositing tin film and particles on the niobium surface to mitigate potential non-uniformity in the coating [11]. These tin deposits act as nucleation sites, which are assumed to grow with the influx of tin vapor during deposition at a higher temperature. The growth temperature should be above 930 °C to exclusively form the Nb_3Sn phase as dictated by the binary phase diagram of the Nb-Sn system [12]. A temperature of about 1100-1200 ºC is typical for Nb_3Sn growth at different labs.

The quality of coated Nb_3Sn layers is contingent on understanding coating layer formation and growth during the process. Several studies have investigated the effect of different coating parameters such as nucleation time, nucleation temperature, growth temperature, growth time, etc., to understand and control the Nb_3Sn growth kinetics [13-14]. Since the essence of the vapor diffusion technique is to create and transport tin gas to the substrate Nb in a suitable thermodynamic environment, the management of Sn during the process is of critical importance. Since many cavities coated recently at Jefferson Lab persistently showed Sn-residues on the coated surface, it further motivated us to correlate Sn effusion conditions, thin-film quality, and RF performance. In this contribution, we discuss several factors that could potentially influence Sn-supply and consumption during the Nb_3Sn film growth affecting the microstructure of the thin film and RF performance.

Nb_3Sn COATING

Each cavity or sample chamber was coated with 10 mm × 10 mm Nb coupon samples inside using a typical setup. The coating deposition system is described in [7]. Sn (99.999% purity from Sigma Aldrich) was loaded in a crucible, and $SnCl_2$ (99.99% purity from Sigma Aldrich) was packaged inside two pieces of Nb foil inside the cavity at the bottom flange. A Nb crucible was used for single-cell cavity coating each time. However, W crucibles of different cross-sectional areas were used for experiments using the sample chamber. Both sides of the cavity or sample chamber were closed with Nb covers by lightly tightening with molybdenum fasteners before installation into the furnace. A typical temperature profile included nucleation step at (540 ± 10) °C for 90 minutes and coating step at (1195± 10) °C for 75 minutes, as shown in Fig. 1. Following a series of experiments, the temperature and coating setup was later modified for single-cell cavity coating.

*Authored by Jefferson Science Associates under contract no. DE¬AC05¬06OR23177
†uttar@jlab.org

ISBN: 978-3-95450-233-2 ISSN: 2673-5504 doi:10.18429/JACoW-SRF2021-TUPTEV013

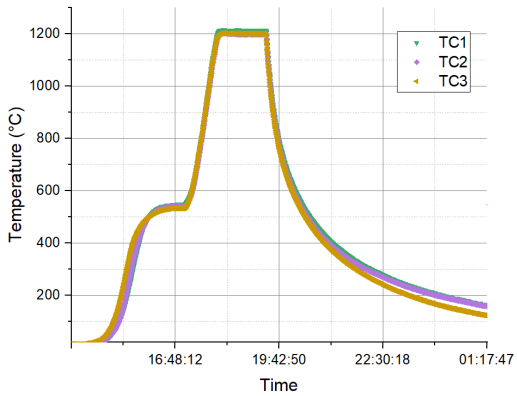

Figure 1: Temperature profile during Nb3Sn coating of a single-cell cavity. TC1, TC2, and TC3 are readings from three thermocouples inside the coating chamber at different locations.

Sn SOURCE AND THIN FILM CHARACTERISTICS

According to the Hertz-Knudsen equation, the maximum molar flux of metal from the condensed form to its gaseous form in a perfect vacuum condition is given by [15]:

$$\dot{\phi} = \frac{P^{\circ}}{\sqrt{2\pi MRT}} \quad (1)$$

where M is the molecular weight, R is the universal gas constant, and T is the absolute temperature at the evaporating surface. $P°$ is the vapor pressure of the metal. Accordingly, we expect the amount of Sn evaporation would be directly proportional to the size of the crucible. For a fixed temperature profile shown in Fig. 1, samples were coated using four different W crucibles with different diameters. A linear relationship was observed between the cross-sectional area and evaporated amount of Sn, as presented in Table 1.

Table 1: Sn Evaporation for Different Crucible Sizes

Crucible	Diameter (inch)	Cross sectional area (cm^2)	Evaporation (g)
D1	1.0	5.07	0.81
D2	0.75	2.85	0.43
D3	0.50	1.27	0.33
D4	0.25	0.32	0.10

The elemental composition and microstructure were examined with a field emission scanning electron microscope (FE-SEM) equipped with an energy-dispersive X-ray spectroscopy (EDS) detector. A set of SEM images from three different crucibles are shown in Fig. 2. It has been observed that the average grain size increased with the increased amount of Sn-supply correlated with a larger crucible for the same period of coating time. For samples coated with crucibles D1 to D3, ~ (24 ± 0.5) at. % Sn was observed. However, only ~21 at. % Sn was observed for the coated with D4, indicating thinner coating where X-ray penetrates below the Nb_3Sn layer. Note that many grains show depression in the middle as expected for the low flux of Sn-supply. With a known correlation between the grain size and roughness, we can expect that larger crucible results in thicker and rougher coatings for the same coating time. Post-coating visual inspection of the crucible indicates typically that a thicker layer of Sn is collected around the corner if any residual Sn is left inside, likely because of the constrained solid angle available due to the depth of each crucible. Application of a shallow crucible may avoid such occurrences.

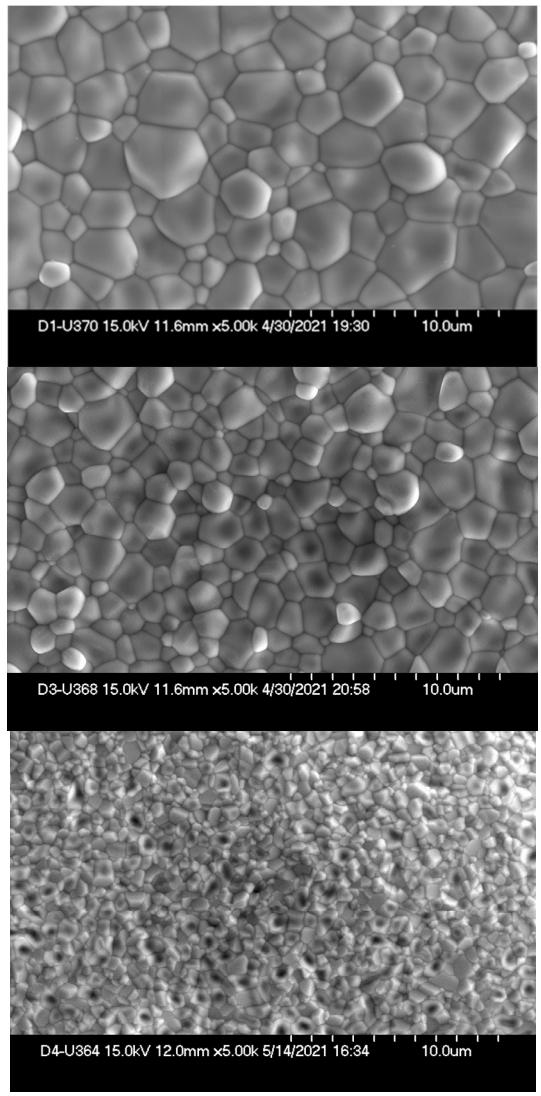

Figure 2: SEM images from samples coated with crucibles with diameters 1 inch, 0.50 inch, and 0.25 inch, respectively.

To further mock a very small amount of Sn-flux during the coating, ~0.5 g Sn was packaged inside a Nb foil instead of a crucible. The SEM image from the sample is shown in Fig. 3, showing irregular grain structures with patchy regions. It depicts the origin of non-uniformity during the coating of large cavities such as multi-cell cavities where the available flux of Sn depletes moving away from the Sn-source. As reported before [16-17], the addition of multiple Sn-sources avoids such a problem.

ISBN: 978-3-95450-233-2 ISSN: 2673-5504 doi:10.18429/JACoW-SRF2021-TUPTEV013

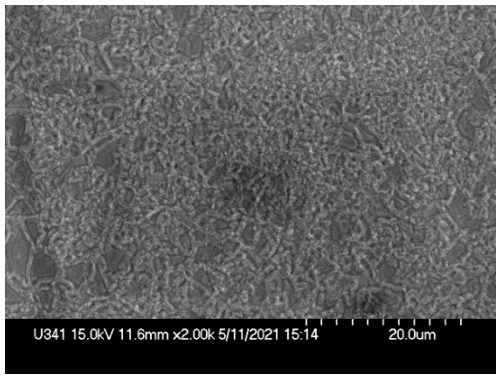

Figure 3: SEM image of the film produced with Sn-restricted inside a Nb foil.

SUBSTRATE AREA AND THIN FILM CHARACTERISTICS

In a typical coating experiment, the assembly is performed inside a cleanroom and transferred to the furnace. Both sides of the cavity or sample chamber are covered with Nb plates to avoid contamination inclusion during the installation into the furnace. The setup is also necessary not to coat the interior of the coating chamber and Sn-condensation into heatshields. The Sn vapor is assumed to be mostly confined inside a cavity during the coating process. A set of experiments were run with identical coating set up and temperature profile to understand how the variation of substrate surface area exposed to Sn-source affects Sn evaporation and then thin film properties. The temperature profile used for this study included three steps at 1200 °C, 1150 °C, and 1100 °C for the film growth, discussed later in the following section. The sample chamber and a cavity of different surface areas were coated in the first two experiments.

The weight loss measurement of the crucible after the coating showed that ~ 85% of the loaded Sn was consumed during a cavity coating compared to only ~ 60% for the sample chamber. About 1 mg.cm^{-2} Sn was consumed during the sample chamber coating, whereas 0.85 mg.cm^{-2} for a single-cell cavity. One end of the sample chamber was left open during the third experiment exposing the Sn source to the coating chamber of the furnace. All the Sn from the crucible was exhausted. SEM pictures in Fig. 4 show the variation in microstructures. Sn evaporating from the source clearly increased with an increase in the exposed surface substrate surface area. In contrast, microstructure variation was dependent on the surface density of Sn during the coating. Comparing coatings with and without an open end of the sample chamber, more Sn was evaporated with an open-end but reduced the grain size, likely with the roughness and thickness as the Sn was no longer confined inside the sample chamber. We had observed residual Sn condensation when both ends of the cavity or the sample chamber, but no such residue was present while one side of the chamber was open during the coating. The size and distribution of nanoscopic residues (not shown here) were decreased as the substrate surface area increased from the sample chamber to the cavity.

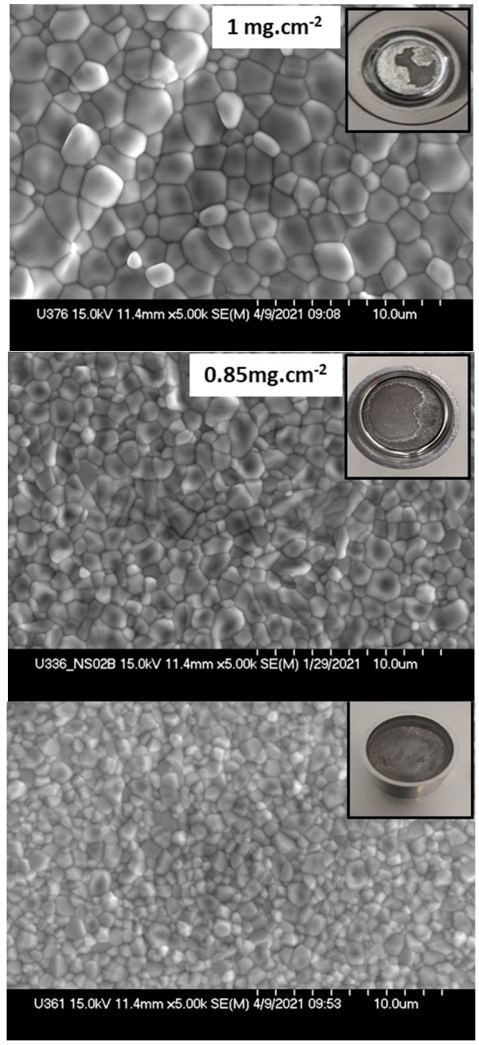

Figure 4: SEM images from sample coated inside (a) closed sample chamber, (b) closed single-cell cavity, and (c) sample chamber with one side open, respectively. Inset pictures show the post-coating appearance of the crucible.

SINGLE-CELL CAVITY COATING

As discussed in the previous section, the coating setup in which the Sn source is in the cavity enclosure during the coating is likely to condense Sn-residue at the end of the coating process. Proper tuning of Sn supply to the cavity surface area may reduce or eliminate residual Sn condensation and engineer suitable surface properties. Two 1.3 GHz single-cell cavities were coated several times with continuous modifications. Those cavities were coated several times where the coating parameters were varied to tune surface characteristics and mitigate Sn-residues. In the past, the standard coating protocol at JLab included three hours at 1200 °C to grow Nb_3Sn coating. Following sample studies, we reduced the growth duration to 75 min aiming for roughness reduction with sufficient thin film thickness for RF interaction, as shown in Fig. 1. The average root mean square roughness (R_q) for 50 µm × 50 µm atomic force microscopy (AFM) scans reduced from (312 ± 39) nm to (202 ± 54) nm. For those cavities, the quench field

ISBN: 978-3-95450-233-2 ISSN: 2673-5504 doi:10.18429/JACoW-SRF2021-TUPTEV013

was >15 MV/m each time but with a Q-slope, as shown in Fig. 5. Note that the quench field was higher than previous coatings where we coated a single cavity and showed Sn-residues [9]. The witness sample had Sn residues ranging in size from a few nm to up to 50 nm (see Fig. 6).

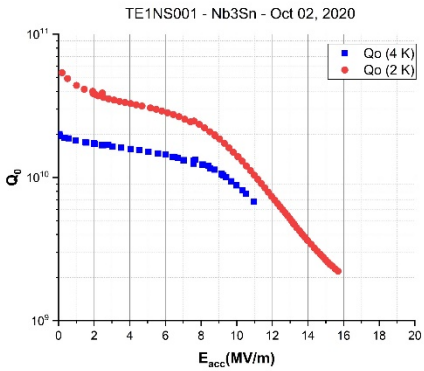

Figure 5: RF Performance of 1.3 GHz single-cell cavity following temperature profile in Fig. 1.

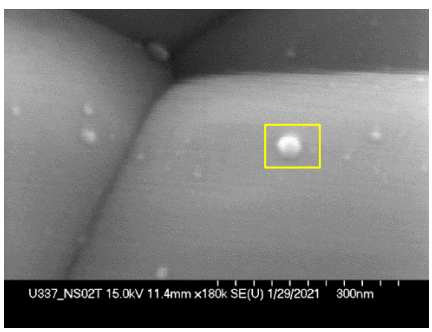

Figure 6: SEM image from witness sample coated with the cavity in Fig. 5. Note that bright features are potential Sn-residues.

The coating setup and the temperature profile were further modified. A half-inch hole was made in the center of the top cover plate. A Nb plug was installed into the hole during the coating assembly, as shown in Fig. 7 (a). It was then attached to the linear bellow drive with a Nb wire on the top multiport plate of the furnace. The goal was to pull out the plug at the end of the heat cycle from outside, releasing Sn vapor from the cavity. The temperature profile was modified as shown in Fig. 7 (b), and the loaded amount of Sn has adjusted accordingly. The short period at 1200 °C was included to ensure a uniform coating grows without any patchy regions with generous Sn-flux. The motivation for the more extended coating with temperature steps at 1150 °C and 1100°C was to gradually lower the Sn-flux at the end of the heat cycle. The temperature profile was estimated to evaporate a lower amount of Sn than the previous heat profile. Samples coated with this profile previously resulted in a smoother coating. The post coating inspection showed that the plug was tilted while loading the cavity into the furnace; that is, a small opening was created next to the plug throughout the process. The cavity was coated uniformly and appeared smoother than the previous run. The Sn consumption was ~ 20% less than that observed with the previous temperature profile.

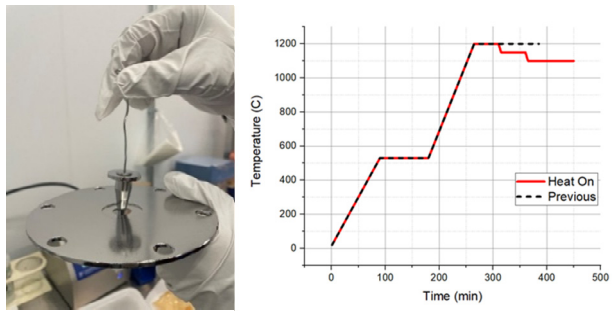

Figure 7: Plug installed in the top plate covering the cavity (left). Schematic diagram depicting the modified temperature profile with three steps (right).

SEM/EDS analysis of the witness sample revealed a uniform coating with a typical Nb_3Sn composition. Despite the reduction in size and density, Sn-residues were present. The average grain size was (0.96 ± 0.06) µm compared to the previous coating with (1.52 ± 0.19) µm. AFM analysis of the witness sample showed R_q of (73±8) nm, significantly lower than the last coating, (202 ± 54) nm, for 50 µm × 50 µm AFM scans. AFM images obtained from cavity witness samples produced with two temperature profiles in Fig. 7 (b) is shown in Fig. 8.

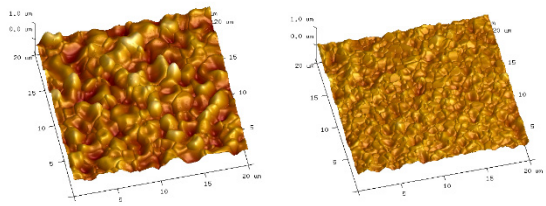

Figure 8: AFM images from witness sample coated with two temperature profiles shown in Figure 7. Note that the second image from the three-step temperature profile for the growth looks visibly smoother.

RF test result from the cavity is summarized in Fig. 9. The low field Q_0 is about 2.5×10^{10} at 4 K and 1×10^{11} at 2 K. A mild Q-slope is present with a quench field ~16 MV/m at 4 K and 17.5 MV/m at 2 K with $Q_0>10^{10}$. We believe that the observed Q-slope is caused by Sn residues present at the surface.

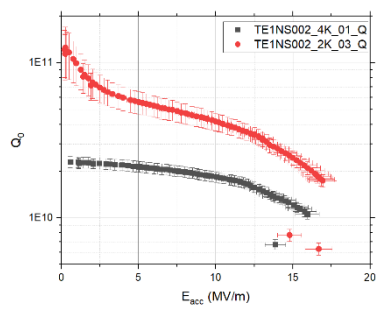

Figure 9: RF results from 1.3 GHz single-cell cavity coated with a three-step temperature profile.

The amount of Sn was further reduced in subsequent cavity coating, aiming for a complete Sn exhaustion. The size of the hole in the top plate was reduced to a quarter-

ISBN: 978-3-95450-233-2 ISSN: 2673-5504 doi:10.18429/JACoW-SRF2021-TUPTEV013

inch in diameter to make sure the plug stays in place. Similar temperature and coating parameters were used. Post coating inspection revealed that all the Sn- was evaporated from the crucible. The cavity looked very similar to the last coating, except some Sn drops splattered into the beam pipe close to the Sn-source. Such spots are examined before and typically have the usual Nb_3Sn composition. SEM examination shows unusual grain faceting but no Sn-residues. (See Fig. 10 (top).) EDS analysis showed the usual composition. AFM image showed similar grain facets and dent-like structures with sharp edges, as shown in, Fig. 10 (bottom). We have noticed similar features developed in Nb_3Sn grains after annealing without Sn before, resulting in severe degradation in RF performance. The estimated average value of R_q is (98±5) nm, slightly rougher than the previous coating, that was (73±8) nm for 50 µm × 50 µm AFM scans. The estimated value for the average grain size was (1.11 ± 0.08) µm.

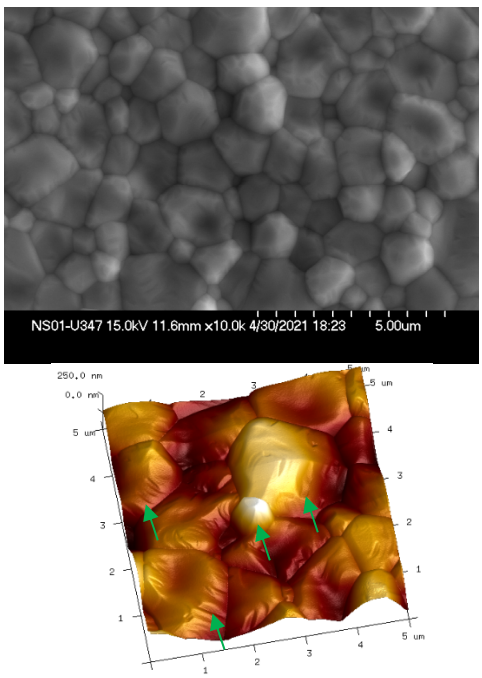

Figure 10: SEM image and AFM image from witness sample resulting by complete Sn-supply exhaustion. Note the sharp edges indicated by arrows and faceting developed in the grain.

RF test at both at 4 K and 2 K is shown in Fig. 11. The low field Q_0 was lower than expected at both temperatures. A slight Q-slope observed at first was followed by a sharp degradation. The cavity was never quenched and was limited by the input power. The sample analysis and the cavity performance behavior were surprisingly consistent with previous cavities that went through extra annealing steps without Sn. Note that besides visible surface degradation with new features with sharp edges, Sn-loss from the coating was observed. A compositional change was not apparent with the EDS analysis here. It seems that Sn-source was exhausted before turning off the heat and annealed for some time without Sn. Potential Sn-loss from the coated layer and an evident surface degradation with the formation of features with sharp edges may explain the observed phenomena of performance degradation.

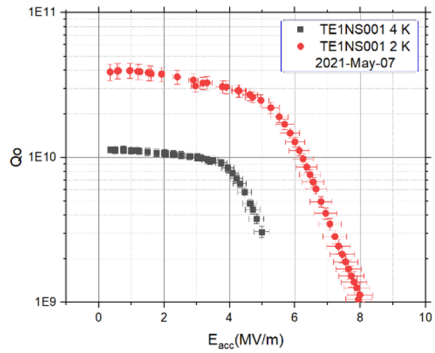

Figure 11: RF result from the cavity with exhausted Sn-source.

Since annealing Nb_3Sn film without Sn seems risky with observed surface degradation, we tried to overcoat some samples with a small amount of Sn, aiming to ensure sufficient vapor pressure not to lose Sn from the coating. Comparing SEM images before and after the overcoat showed significantly improved surface without "annealing" features, as shown in Fig. 12.

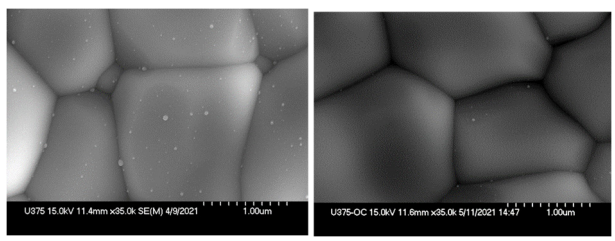

Figure 12: SEM image of the sample before (left) and after (right) overcoat with a small amount of Sn supplied inside a Nb foil. Note that most of the residues are absent after the overcoat.

SUMMARY AND OUTLOOK

We investigated several factors that could potentially influence Sn supply and consumption during the Nb_3Sn film growth, affecting the thin film's microstructure and RF performance. Besides the temperature profile, the crucible size and the exposed substrate area need careful consideration tuning of the surface properties of the coating. It is essential to have generous tin flux at the initial stage to grow uniformly, and it is equally important to make sure not to anneal the coating without Sn to avoid film degradation. More careful material analysis is in progress to correlate RF performance with different coating conditions discussed above. We are updating the coating setup and temperature profile to eliminate Sn-residue and to further tune surface characteristics.

ACKNOWLEDGMENTS

We are grateful to Olga Trifimova for her help with AFM analysis. SEM/EDS and AFM measurement was done at

ISBN: 978-3-95450-233-2 ISSN: 2673-5504 doi:10.18429/JACoW-SRF2021-TUPTEV013

Applied Research Center Core Labs, College of Willam & Mary.

REFERENCES

[1] H. Padamsee *et al*., *RF Superconductivity for Accelerators, 2nd Ed.* New York, USA: Wiley & Sons, 1998.

[2] Arnolds, G. and Proch, D., "Measurement on a Nb3Sn structure for linear accelerator application," *IEEE Trans. Magn.*, vol. 13, no. 1, pp.500-503, 1977. doi: 10.1109/TMAG.1977.1059387

[3] P. Kneisel *et al*., "Measurements of superconducting Nb3Sn cavities in the GHz range," in *IEEE Trans. Magn.*, vol. 15, no. 1, pp. 21-24, January 1979, doi: 10.1109/TMAG.1979.1060193.

[4] P. Kneisel *et al.,* "Nb3Sn Layers on High-Purity Nb Cavities with Very High Quality Factors and Accelerating Gradients", in *Proc. 5th European Particle Accelerator Conf. (EPAC'96),* Sitges, Spain, Jun. 1996, paper WEP002.

[5] R. D. Porter *et al*., "Next Generation Nb3Sn SRF Cavities for Linear Accelerators", in *Proc. 29th Linear Accelerator Conf. (LINAC'18)*, Beijing, China, Sep. 2018, pp. 462-465. doi:10.18429/JACoW-LINAC2018-TUPO055

[6] S. Posen et al., "Development of Nb3Sn Coatings for Superconducting RF Cavities at Fermilab," No. FERMILAB-CONF-18-477-TD. Fermi National Accelerator Laboratory (FNAL), Batavia, IL (United States), 2018. https://www.osti.gov/biblio/1480475-development-nb3sn-coatings-superconducting-rf-cavities-fermilab

[7] G. Eremeev *et al.,* "Nb3Sn multi-cell cavity coating system at Jefferson Lab." *Rev. Sci. Instrum.,* vol. 91, no. 7, p. 073911, 2020. doi: 10.1063/1.5144490

[8] Z. Q. Yang *et al.,* "Development of Nb_3Sn Cavity Coating at IMP", in *Proc. 19th Int. Conf. RF Superconductivity (SRF'19)*, Dresden, Germany, Jun.-Jul. 2019, pp. 21-24. doi:10.18429/JACoW-SRF2019-MOP003

[9] U. Pudasaini *et al.,* "Nb_3Sn Films for SRF Cavities: Genesis and RF Properties", in *Proc. 19th Int. Conf. RF Superconductivity (SRF'19)*, Dresden, Germany, Jun.-Jul. 2019, pp. 810-817. doi:10.18429/JACoW-SRF2019-THFUA6.

[10] S. Posen *et al.,* "Advances in Nb_3Sn superconducting radiofrequency cavities towards first practical accelerator applications." *Supercond. Sci. Tech.* vol. 34, p. 025007, 2021. doi:10.1088/1361-6668/abc7f7

[11] Pudasaini, Uttar *et al*., "Initial growth of tin on niobium for vapor diffusion coating of Nb_3Sn." *Supercond. Sci. Technol.* vol. 32, no. 4, p. 045008, 2019. doi:10.1088/1361-6668/aafa88

[12] J.P.Charlesworth *et al.,* "Experimental work on the niobium-tin constitution diagram and related studies." *J. Mater Sci,* vol.5, no. 7, pp. 580-603, 1970. doi:10.1007/BF00554367

[13] U. Pudasaini *et al*. "Growth of Nb_3Sn coating in tin vapor-diffusion process." *J. Vac. Sci. Technol. A*, vol. 37, no. 5, p. 051509, 2019. doi: 10.1116/1.5113597

[14] S. Posen & D. L. Hall, "Nb_3Sn superconducting radiofrequency cavities: fabrication, results, properties, and prospects," *Supercond. Sci. Technol.*, vol. 30, no. 3, p. 033004, 2017 doi:10.1088/1361-6668/30/3/033004

[15] Igor Bello, *Vacuum and Ultravacuum: Physics and Technology.* CRC Press, 2017.

[16] G. V. Eremeev *et al.,* "Insights Into Nb_3Sn Coating of CEBAF Cavities From Witness Sample Analysis", in *Proc. 19th Int. Conf. RF Superconductivity (SRF'19)*, Dresden, Germany, Jun.-Jul. 2019, pp. 60-64. doi:10.18429/JACoW-SRF2019-MOP016

[17] T. Spina *et al*., "Development and Understanding of Nb_3Sn films for radiofrequency applications through a sample-host 9-cell cavity," *Supercond. Sci. Technol.*, vol. 34, p. 015008, 2020. doi:10.1088/1361-6668/abbec4